Article

Catalytic Intermolecular Carboamination of Unactivated Alkenes via Directed Aminopalladation

Zhen Liu, Yanyan Wang, Zichen Wang, Tian Zeng, Peng Liu, and Keary M. Engle

J. Am. Chem. Soc., **Just Accepted Manuscript** • DOI: 10.1021/jacs.7b06520 • Publication Date (Web): 20 Jul 2017

Catalytic Intermolecular Carboamination of Unactivated Alkenes via Directed Aminopalladation

Zhen Liu,[†] Yanyan Wang,[‡] Zichen Wang,[†] Tian Zeng,[†] Peng Liu,*[,‡] Keary M. Engle*[,†]

[†]Department of Chemistry, The Scripps Research Institute, 10550 North Torrey Pines Road, La Jolla, California 92037, United States

[‡]Department of Chemistry, University of Pittsburgh, Pittsburgh, Pennsylvania 15260, United States

Supporting Information Placeholder

ABSTRACT: An intermolecular 1,2-carboamination of unactivated alkenes proceeding via a Pd(II)/Pd(IV) catalytic cycle has been developed. To realize this transformation, a cleavable bidentate directing group is used to control the regioselectivity of aminopalladation and stabilize the resulting organopalladium(II) intermediate, such that oxidative addition to a carbon electrophile outcompetes potential *β*-hydride elimination. Under the optimized reaction conditions, a broad range of nitrogen nucleophiles and carbon electrophiles were compatible coupling partners in this reaction, affording moderate to high yields. The products of this reaction can be easily converted to free γ-amino acids and γ-lactams, both of which are common structural motifs found in drug molecules and bioactive compounds. Reaction kinetics and DFT calculations shed light on the mechanism of the reaction and explain empirically observed reactivity trends.

INTRODUCTION

Nitrogen-containing small molecules possess diverse bioactivity and are commonly encountered as pharmaceutical agents, agrochemicals, and natural products.[1] 1,2-Carboamination of alkenes offers a potentially powerful platform for accessing structurally complex amines from comparatively common and inexpensive starting materials. However, despite extensive effort over the past decades, realizing a catalytic intermolecular carboamination of unactivated alkenes has remained a challenge. During the last decade, Wolfe and others have developed a series of palladium(0)-catalyzed intramolecular carboamination methods by using alkene substrates with a tethered nitrogen nucleophile (Scheme 1A).[2] These transformations are an effective means of accessing various azaheterocycles. A significant advance was reported in 2015 by Piou and Rovis using rhodium(III) as a catalyst to promote coupling of an enoxyphthalimide (which serves as both the nitrogen and carbon source) with an electronically activated alkene. (Scheme 1B).[3] Three-component intermolecular carboamination reactions that proceed with unactivated alkenes would be highly enabling but remain underdeveloped.[3,4]

Based on our previous success in palladium(II)-catalyzed alkene hydrofunctionalization[5,6] and 1,2-dicarbofunctionalization,[7] we questioned whether a chelation-stabilized aminopalladated Wacker-type intermediate could be intercepted with a carbon electrophile as a strategy for alkene carboamination.[8,9] By strategic use of a proximal removable directing group to control the regioselectivity of aminopalladation and stabilize the resulting alkylpalladium(II) intermediate, we envisioned that we could develop a highly selective and heretofore elusive three-component carboamination reaction via a Pd(II)/Pd(IV) catalytic cycle (Scheme 1C). To the best of our knowledge, palladium(II)-catalyzed intermolecular three-component carboamination of unactivated alkenes is unprecedented.[10] Herein, we describe a new catalytic carboamination method for unactivated alkene substrates, wherein a removable bidentate directing group enables regioselective aminopalladation and facilitates subsequent oxidative addition and reductive elimination. This method enables straightforward access to drug molecules and natural products bearing γ-amino acid and γ-lactam structural motifs and is amenable to combinatorial synthesis (Scheme 1D).

Scheme 1. Background and Project Synopsis

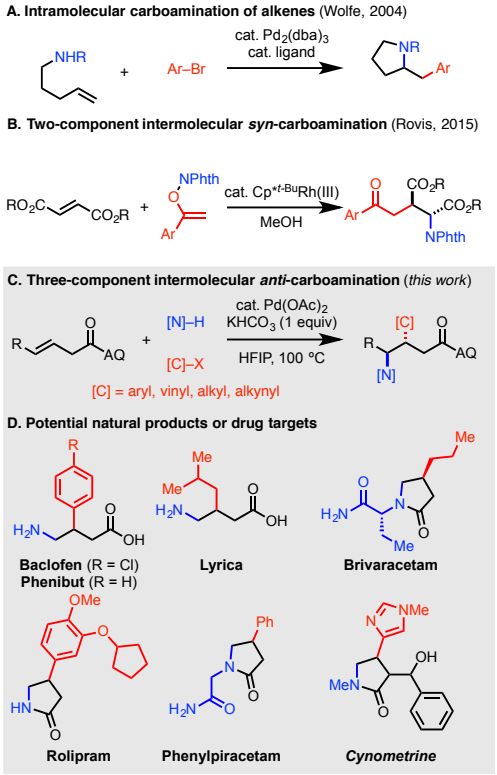

RESULTS AND DISCUSSION

To initiate our study, 3-butenoic acid masked as the corresponding 8-aminoquinoline (AQ)[9a,b,f] amide (**1a**) was selected as the pilot alkene substrate, and phthalimide (**2a**) and 4-iodoanisole (**3q**) were investigated as potential coupling partners. During initial screening, we were delighted to find that 23% of the desired product was formed by using 10 mol% $Pd(OAc)_2$ as the catalyst and 1 equiv K_2CO_3 as the base in toluene as solvent (Table 1, entry 1). Different inorganic bases were tested (entries 1–3), and K_2HPO_4 gave the highest yield (up to 34%) in toluene. We then discovered that when hexafluoroisopropanol (HFIP) was used as solvent, the yield increased to 44% (entry 6). Further optimization revealed that lowering temperature to 100 °C and

switching the inorganic base to $KHCO_3$ gave a higher yield of 54% (entry 8). Finally, we found that by increasing the amount of the 4-iodoanisole (**3q**) to 6 equiv, the 1,2-aminoarylated product **4q** was generated in 61% yield (entry 10). Gratifyingly, when we tested the more reactive electrophile styrenyl iodide (**3a,** 4 equiv), the corresponding aminovinylated product **4a** was isolated in 85% yield under the optimized reaction conditions (entry 11).

Table 1. Optimization of the Reaction Conditions[a]

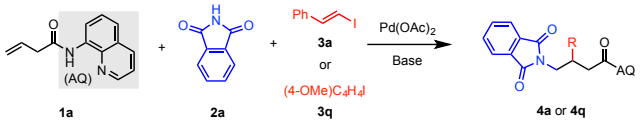

entry	Electrophile	Solvent	Base	Temp. (°C)	Yield[b] (%)
1	**3q**	toluene	K_2CO_3	110	(23)
2	**3q**	toluene	Cs_2CO_3	110	trace
3	**3q**	toluene	K_2HPO_4	110	(34)
4	**3q**	MeCN	K_2HPO_4	110	trace
5	**3q**	DCE	K_2HPO_4	110	(7)
6	**3q**	HFIP	K_2HPO_4	110	(44)
7	**3q**	HFIP	$KHCO_3$	110	38
8	**3q**	HFIP	$KHCO_3$	100	54
9	**3q**	HFIP	K_2HPO_4	100	(15)
10[c]	**3q**	**HFIP**	**$KHCO_3$**	**100**	**61**
11	**3a**	**HFIP**	**$KHCO_3$**	**100**	**85**

[a]Reaction conditions: **1a** (0.1 mmol), **2a** (1.5 equiv), **3a** or **3q** (4 equiv), $Pd(OAc)_2$ (10 mol %), base (1 equiv), HFIP (0.2 mL), air, 10–24 h. [b]Isolated yield. Values in parentheses represent yields determined by ^{1}H NMR analysis of the crude reaction mixture using CH_2Br_2 as internal standard. [c]6 equiv of aryl iodide **3q**.

Having optimized the reaction conditions, we next investigated the substrate scope of this palladium(II)-catalyzed alkene carboamination reaction. First, various carbon electrophiles were tested with alkene substrate **1a** and phthalimide (**2a**) as the nitrogen nucleophile (Table 2). An array of *E*- and *Z*-styrenyl iodides containing different substituents on the aromatic ring were found to be reactive, providing the corresponding carboaminated products in moderate to high yields (**4a**–**4e**). Notably, bromide and chloride groups were tolerated, presenting the opportunity for subsequent diversification via cross-coupling. A 2-thienyl group was well tolerated on the alkenyl iodide (**4f**), and a 1-iodo-1,3-diene was similarly competent as a reaction partner (**4g**). Several alkyl-substituted alkenyl iodides were also suitable electrophiles in this transformation (**4h**–**4n**), including a 2,2-dimethyl-substituted example (**4k**). In general, alkenyl iodides bearing a substituent at the 1-position were inefficient coupling partners in this reaction, presumably due to steric hindrance, which increases the activation energy for the oxidative addition and reductive elimination steps. Fortunately, 1-iodo-cycloheptene was found to be an exception, and we were able to obtain carboaminated product **4l** in 70% yield. Surprisingly, the presence of a free hydroxyl group was well tolerated (**4m**), as were the ether and ester groups in the steroid-derived alkenyl iodide (**4n**). With *E*-alkenyl iodides, the reaction was completely stereoretentive in terms of alkene geometry, whereas with *Z*-alkenyl iodides, there was noticeable erosion of the *Z*-stereochemistry in the product compared to the starting material (**4d**–**4g** and **4j**).[11]

Table 2. Carbon Electrophile Scope[a]

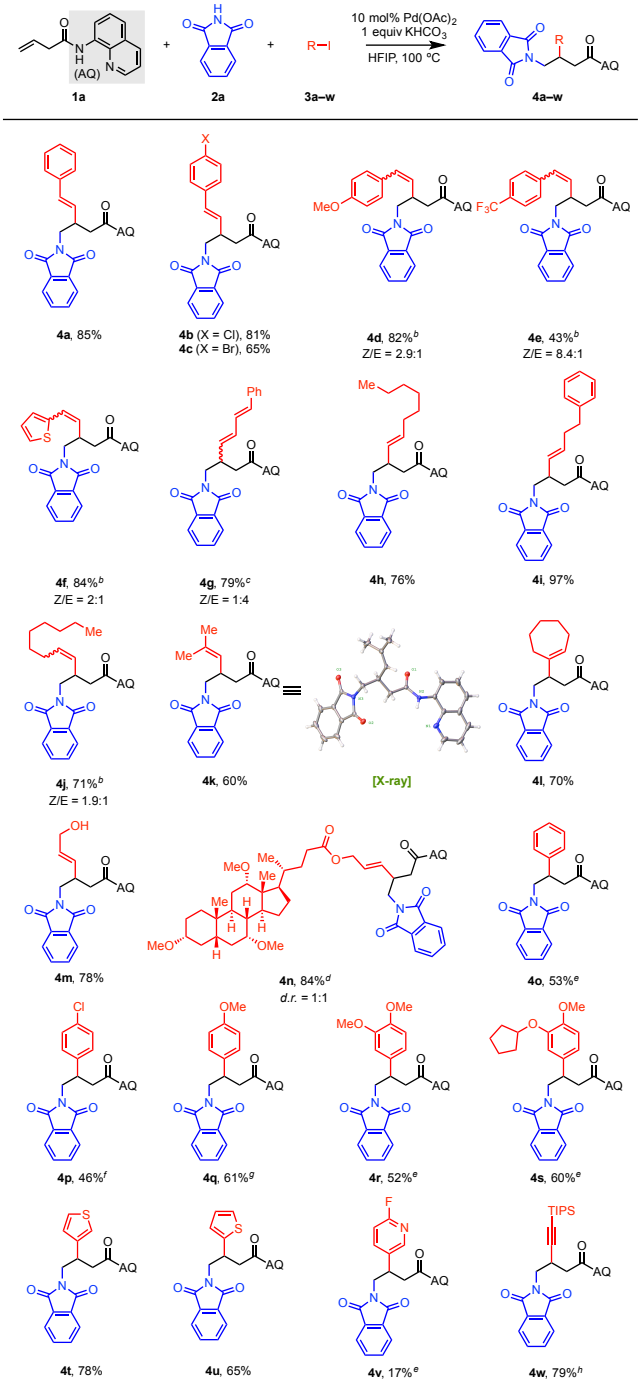

[a]Reaction conditions: **1a** (0.1 mmol), **2a** (1.5 equiv), electrophile (4 equiv), $Pd(OAc)_2$ (10 mol %), $KHCO_3$ (1 equiv), HFIP (0.2 mL), 100 °C, air, 10–24 h. Percentages refer to isolated yields. [b]Pure (*Z*)-alkenyl iodide was used. *Z*/*E* ratios were determined by ^{1}H NMR analysis of the crude reaction mixtures and were consistent with those of the purified products. [c]Alkenyl iodide **3g** was used as a mixture of *Z*/*E* isomers (*Z*/*E* = 1.6:1). [d]Enantiopure alkenyl iodide **3n** was used. [e]8 equiv of aryl iodide, 48 h. [f]10 equiv of 1-chloro-4-iodobenzene (**3p**), 72 h. [g]6 equiv of 4-iodoanisole (**3q**). [h](Bromoethynyl)triisopropylsilane (**3w**) was used as the electrophile.

Aryl iodides were also competent electrophiles, and substituents on the *para* or *meta* position were tolerated under the optimized conditions, with electron-withdrawing groups attenuating reactivity (**4o**–**4s**). Heteroaryl iodides, bearing a thienyl group (**3t** and **3u**), are excellent coupling partners in this reaction. While pyridine-based aryl iodides are not very reactive under the standard condition, requiring a substituent at 2-position to diminish the pyridine nitrogen coordination (**4v**). In general, aryl iodides were less reactive in this transformation, requiring additional equivalents to achieve moderate yields. Additionally, we managed to install an alkynyl group by using (bromoethynyl)triisopropylsilane (**3w**) as the electrophile in good yield (**4w**). In general, alkenyl iodides and (bromoethynyl)triisopropylsilane were the most reactive electrophiles, followed by electron-rich aryl iodides, and finally electron-poor aryl iodides (*vide infra*), similar to the trend that was observed in our previously published 1,2-dicarbofunctionalization.[7]

We next moved on to examine alkyl iodides as potential electrophiles in this reaction (Table 3). Notably, in our previously reported 1,2-dicarbofunctionalization, we were unable to achieve even modest yield with any alkyl iodide coupling partners.[7] In contrast, under optimal carboamination conditions, when using methyl iodide (**3x**) as the electrophile, the 1,2-aminomethylated product was formed in moderate yield. Unfortunately, this result was not general to other alkyl iodides, potentially due to steric considerations, as other alkyl iodides were incapable of providing the desired products (**4z**–**4ab**). Among many that were tested (selected examples of which are shown in Table 3) only 2-iodoacetonitrile (**3y**) was found to participate in the reaction, giving 11% of **4y**. Though these results are preliminary in nature, they nevertheless establish the viability of achieving $C(sp^3)$–$C(sp^3)$ bond formation in the final reductive elimination step in 1,2-alkene difunctionalization via Pd(II)/Pd(IV) catalysis.

Table 3. Alkyl Electrophile Scope[a]

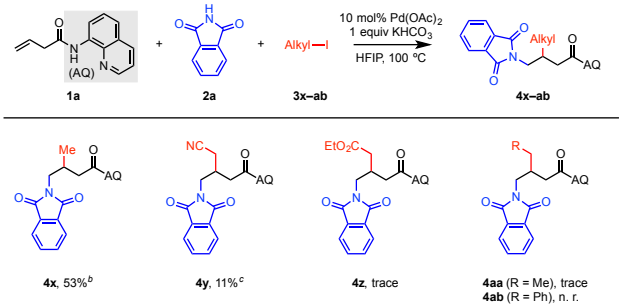

[a]Reaction conditions: **1a** (0.1 mmol), **2a** (1.5 equiv), **3x–ab** (4 equiv), $Pd(OAc)_2$ (10 mol %), $KHCO_3$ (1 equiv), HFIP (0.2 mL), 100 °C, air, 10–24 h. Percentages refer to isolated yields. [b]75 % conversion. [c]48% conversion.

Next, the scope of nitrogen nucleophiles was studied with alkene substrate **1a** and styrenyl iodide (**3a**) or 4-iodoanisole (**3q**) as the electrophile under the standard reaction conditions (Table 4). First, different masked ammonia nucleophiles that can easily be converted to primary amines upon deprotection were tested. To our delight, many 5- and 6-membered cyclic imides all underwent carboamination in excellent yields (**5a**–**5d**), including the commercial immunomodulatory drug thalidomide (**5c**). Tosyl- and nosyl-protected amines (**2f** and **2g**) were also competent nucleophiles but gave lower yields (**5e** and **5f**). Additionally, the reaction performed smoothly with hydroxamic acid derivatives (**5g** and **5h**). Importantly, several azaheterocycles, relevant to medicinal chemistry,[1b] including triazole (**2k**), benzimidazole (**2l**) and carbazole (**2m**), were also suitable nucleophiles in this reaction (**5j**–**5m**).

Table 4. Nitrogen Nucleophile Scope[a]

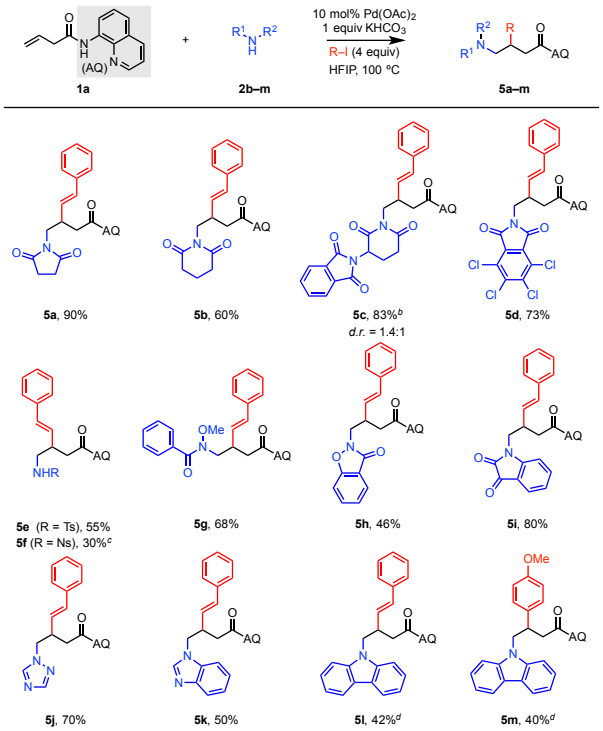

[a]Reaction conditions: **1a** (0.1 mmol), **2b–m** (1.5 equiv), electrophile (4 equiv), $Pd(OAc)_2$ (10 mol %), $KHCO_3$ (1 equiv), HFIP (0.2 mL), 100 °C, air, 10–24 h. All the yields refer to the isolated yields. [b]Thalidomide was used as the nucleophile. [c]75% conversion. [d]1 equiv of K_2CO_3, toluene (0.2 mL), 110 °C.

Subsequently, we examined the scope of unactivated alkenes with phthalimide (**2a**) as the nucleophile and styrenyl iodide (**3a**) as the electrophile. We were pleased to find that internal alkene (*E*)-**1b** could be successfully converted into carboaminated product, although in relatively low yield. Though stereochemically pure (*E*)-alkene was used in the reaction, the diastereomeric ratio of **6a** was observed to be approximately 1.1:1. This is likely due to rapid *E*/*Z* isomerization of the alkene substrate under the reaction conditions.[12] Cyclopentenyl substrate **1c** was also carboaminated under the standard conditions. Notably, this transformation establishes two new stereocenters and provides expedient access to a highly substituted cyclopentane framework. The *trans* relationship of the two new substituents is consistent with *anti*-nucleopalladation[7] and stereoretentive oxidative addition/reductive elimination.[9f] A variety of α-substituted terminal alkenes were found to be suitable substrates and underwent carboamination in moderate to high yields (**6c**–**6g**). The steric properties of the α-substituent have a dramatic effect on the diastereoselectivity. α-Methyl substituted carboamination product **6c** was formed in a diastereomeric ratio of only 5:1. With more sterically demanding isopropyl or benzyl groups, the diastereomeric ratios of corresponding products are greater than 20:1 (**6d** and **6e**). The relative stereochemistry of **6e**, as determined by X-ray crystallography, is consistent with selective formation of a *trans* 5-membered palladacycle intermediate upon nucleopalladation.[7] With a substrate containing two alkenes, the reaction proved to be chemoselective in preferentially functionalizing the proximal β-γ alkene over the more distal δ-ε alkene

(**6f** and **6g**) because only the former can react to give a 5-membered palladacycle. Carboamination of the sterically congested α,α-disubstituted alkene substrate proceeded in a relatively good yield, albeit at a slower rate, requiring longer reaction time (**6h**).

Table 5. Unactivated Alkene Scope[a]

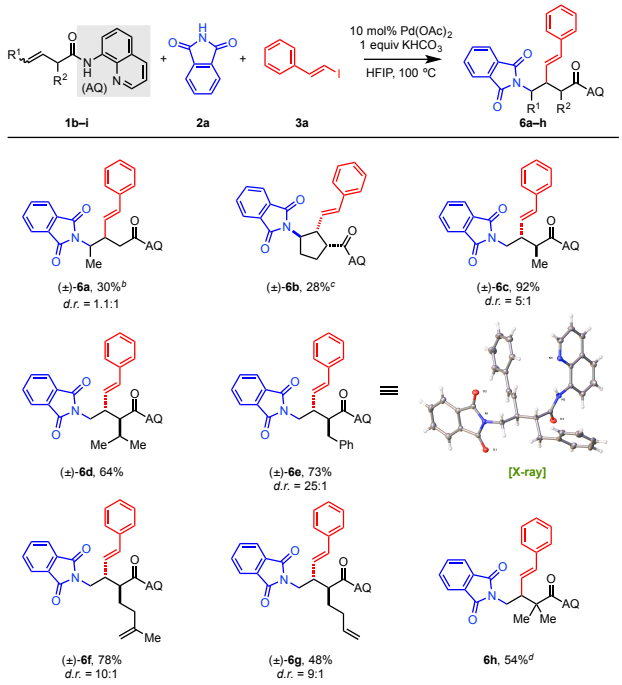

[a]Reaction conditions: **1b–i** (0.1 mmol), **2a** (1.5 equiv), **3a** (4 equiv), $Pd(OAc)_2$ (10 mol %), $KHCO_3$ (1 equiv), HFIP (0.2 mL), 100 °C, air, 10–24 h. All the yields refer to the isolated yields. [b]64% conversion. [c]61% conversion. [d]34 h. 70% conversion.

Upon removal of the AQ directing group (and amine deprotection when necessary), the products of this reaction are functionalized γ-amino acids, which are ubiquitous core structures in human therapeutics. To demonstrate the practical utility of this Pd(II)-catalyzed alkene carboamination method as a tool for library synthesis in the context of drug discovery, we performed the synthesis of a number of commercially available drug molecules and their derivatives bearing a structure motif of γ-amino acid or γ-lactam (Scheme 2). Notably, all of these compounds were synthesized from a common alkene substrate, **1a**, and a single nitrogen nucleophile, phthalimide (**2a**). Lyrica, which is used both as an anticonvulsant and to treat general anxiety disorder,[13] was synthesized in 5 steps with an overall yield of 47%. Baclofen, used to treat spasticity,[14] and phenibut, utilized for its anxiolytic effects,[15] were both obtained in moderate yields in two steps. Rolipram, an anti-inflammatory API,[16] and its derivative **7** were also prepared efficiently. To demonstrate the scalability and operational simplicity of the carboamination reaction, the first steps of lyrica and rolipram derivative **7** syntheses were carried out on 2 mmol scale.

Scheme 2. Synthesis of Drugs and Their Derivatives[a]

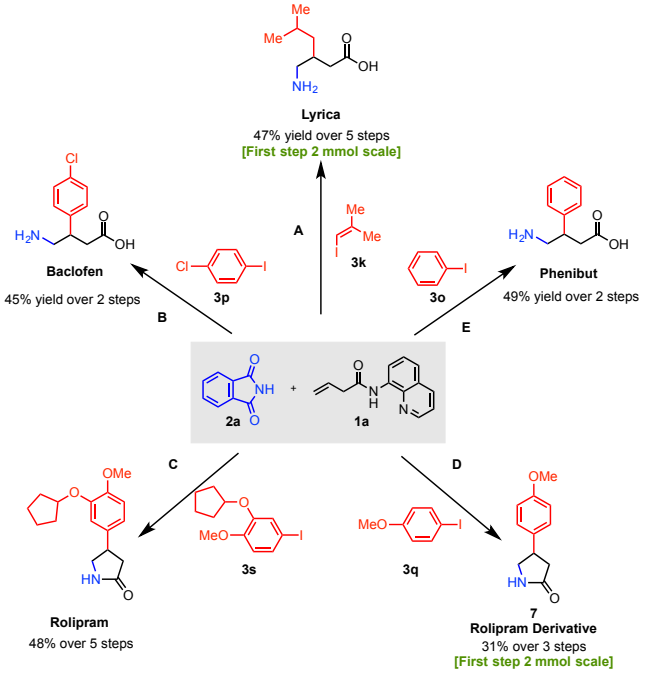

[a]Reagents and conditions: (**A**, Step 1) **1a** (2 mmol), **2a** (1.5 equiv), **3k** (4 equiv), $Pd(OAc)_2$ (10 mol %), $KHCO_3$ (1 equiv), HFIP (4 mL), 100 °C, 36 h, 65%; (**A**, Step 2) Boc_2O (10 equiv), DMAP (2.5 equiv), THF, 50 °C, 3 h; (**A**, Step 3) $LiOH•H_2O$ (1.1 equiv), H_2O_2 (8.8 equiv), THF/H_2O (3:1), 0 °C, 2.5 h, 97% (2 steps); (**A**, Step 4) Pd/C (10 mol%), H_2 (20 atm), EtOAc, 23 °C, 60 h; (**A**, Step 5) HCl (6 M), 130 °C, 24 h, 75% (2 steps). (**B**, Step 1) **1a** (0.1 mmol), **2a** (1.5 equiv), **3p** (10 equiv), $Pd(OAc)_2$ (10 mol %), $KHCO_3$ (1 equiv), HFIP (0.2 mL), 100 °C, 72 h, 46%; (**B**, Step 2) HCl (6 M), 130 °C, 24 h, 97%. (**C**, Step 1) **1a** (0.1 mmol), **2a** (1.5 equiv), **3s** (8 equiv), $Pd(OAc)_2$ (10 mol %), $KHCO_3$ (1 equiv), HFIP (0.2 mL), 100 °C, 48 h, 60%; (**C**, Step 2) Boc_2O (10 equiv), DMAP (2.5 equiv), THF, 50 °C, 3 h; (**C**, Step 3) $LiOH•H_2O$ (1.1 equiv), H_2O_2 (8.8 equiv), THF/H_2O (3:1), 0 °C, 2.5 h, 89% (2 steps); (**C**, Step 4) $N_2H_4•H_2O$ (4 equiv), MeOH, 23 °C, 24 h; (**C**, Step 5) $SOCl_2$/MeOH (1:10), 23 °C, 12 h; then NaOH (2 M), 23 °C, 1 h, 90% (2 steps). (**D**, Step 1) **1a** (2 mmol), **2a** (1.5 equiv), **3q** (6 equiv), $Pd(OAc)_2$ (10 mol %), $KHCO_3$ (1 equiv), HFIP (4 mL), 100 °C, 24 h, 61%; (**D**, Step 2) HCl (6 M), 130 °C, 24 h; (**D**, Step 3) Al_2O_3 (2 equiv), toluene, 125 °C, 24 h, 50% (2 steps). (**E**, Step 1) **1a** (1 mmol), **2a** (1.5 equiv), **3o** (8 equiv), $Pd(OAc)_2$ (10 mol %), $KHCO_3$ (1 equiv), HFIP (2 mL), 100 °C, 48 h, 52%; (**E**, Step 2) HCl (6 M), 130 °C, 24 h, 95%.

MECHANISTIC ANALYSIS

Similar to our previously published 1,2-dicarbofunctionalization,[7] three mechanistic scenarios could be imagined for this catalytic alkene 1,2-carboamination reaction (Scheme 3). Pathway A involves aminopalladation to form a five-membered palladacycle followed by direct reaction of this alkylpalladium(II) intermediate with the organohalide via oxidative addition to palladium(IV) and reductive elimination to generate the carboaminated product. Pathway B similarly begins with aminopalladation, but in this case, rapid and reversible protodepalladation then takes place to form a hydroaminated intermediate.[5] This intermediate can reengage with the catalyst and undergo C–H cleavage to reform the palladacycle. In this case, the hydroaminated intermediate would be favored at equilibrium, making it distinct from Pathway A. An additional plausible mechanistic pathway (Pathway C) involves aza-Wacker addition into the alkene with subsequent β-H elimination to generate Pd(0) and the

corresponding enamine, oxidative addition of Pd(0) to the organohalide, Heck-type carbopalladation to give a six-membered palladacycle, and finally protodepalladation of the resultant alkylpalladium(II) species to form the product.

To probe the viability of these pathways, several mechanistic experiments were performed (Scheme 4). In the first experiment, we subjected alkene substrate **1a** and phthalimide (**2a**) to the reaction conditions in the absence of the electrophile. In this case, only 8% of the putative hydroaminated intermediate **8** was observed (Scheme 4A). Notably, in the ^{1}H NMR kinetic studies of this 1,2-carboamination reaction described below, we have also observed that **8** does not build up at any point during the course of the reaction. In the second experiment, we independently prepared **8**[5] and used this compound in place of the alkene in the standard reaction without additional nucleophile (Scheme 4B). No product was observed in this experiment. The former result illustrates that protodepalladation to form **8** is not facile under these reaction conditions. The latter result establishes that the requisite C–H alkenylation process in Pathway B does not take place under these reaction conditions.[17] Next, we took note of the connectivity of α-methyl product **6c** and α,α-*gem*-dimethyl product **6h**; if Pathway B were operative, one would expect the alkenyl group to be installed at the α-methyl position since palladium(II) species are known to preferentially activate methyl C(sp^3)–H bonds rather than methylene C(sp^3)–H bonds.[9e,f] Similarly, with other substrates in Table 5 that contain α-alkyl branching, regioisomeric product mixtures would be expected if C–H alkenylation were operative. Collectively, these results are inconsistent with Pathway B. In a third experiment, we prepared deuterium-labeled substrate d_2-**1a** and subjected it to the standard conditions (Scheme 4C). No H/D exchange in the product was observed, suggesting that β-hydride/deuteride elimination does not take place at the terminal position. Additionally, β-hydride elimination intermediates were not observed during ^{1}H NMR kinetic experiments. These results are inconsistent with Pathway C. Overall, the experiments depicted in Scheme 4 are consistent with Pathway A and inconsistent with the other two possible mechanisms.

Scheme 3. Possible Mechanistic Pathways for Alkene Carboamination

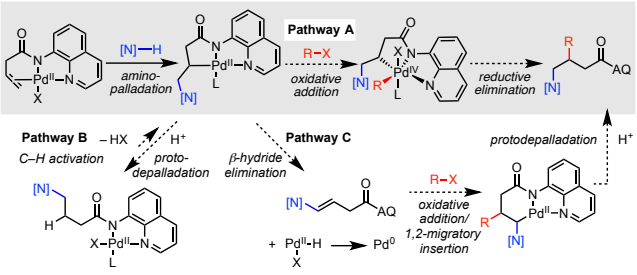

We next performed Reaction Progress Kinetic Analysis (RPKA), which is a powerful method for interrogating the mechanism of complex catalytic processes.[18] First, we established a reproducible standard protocol using alkene **1a**, phthalimide (**2a**), and alkenyl iodide **3i** using 1,3,5-triisopropylbenzene as internal standard. Aliquots were removed at predetermined time points, diluted with $CDCl_3$, and monitored by ^{1}H NMR.

Scheme 4. Mechanistic Study

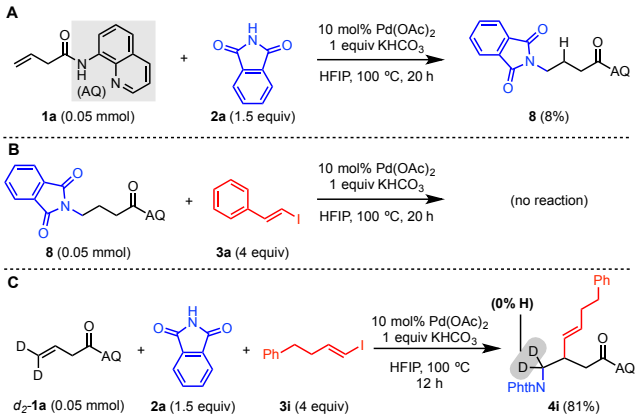

At the outset, we were aware that the multicomponent nature of this reaction could potentially lead to complicated kinetic behavior. In terms of general features of the reaction, the kinetic data that we describe below suggests that the reaction has two regimes, one at less than approximately 50% conversion (roughly five catalyst turnovers), and one at higher conversion. Several different causes could explain this phenomenon, including catalyst deactivation, product inhibition, change in pH, or precipitation of reaction components at high conversion. Because the first regime is more likely to reflect the intrinsic kinetics of the catalytic system, the remainder of the discussion will focus on this portion of the reaction. Though it could be potentially interesting in its own right, a detailed investigation of the second regime is outside of the scope of the present investigation. We also note that the reaction has an induction period of approximately 10 min. During this time, formation of the corresponding alkene-bound Pd(II) complex[5] can be observed by ^{1}H NMR of reaction aliquots.[19] In the ensuing analysis, we define 'excess' $[e]$ of one reaction component over another as the difference in their initial molarities, in particular:

$$[\mathbf{2a}]_0 = [\mathbf{1a}]_0 + [e]_{\mathbf{2a}}$$

$$[\mathbf{3i}]_0 = [\mathbf{1a}]_0 + [e]_{\mathbf{3i}}$$

Two same-excess experiments were carried out with 0.5 and 0.8 equiv of alkene **1a** (Figures 1A and Figure S5B). A same-excess experiment simulates entering the reaction after a certain amount of starting material has been consumed (*i.e.*, a certain number of catalyst turnovers). Rate profiles of a standard run and a same-excess experiment are expected to overlay if the on-cycle catalyst concentrations are equivalent in both cases. In our experiments, the data from both same-excess experiments were found to overlay with the standard rate profile when time-adjusted, indicating that there is no significant catalyst deactivation or product inhibition in this reaction.

A

	$[\mathbf{1a}]_0$ (M)	$[\mathbf{2a}]_0$ (M)	$[e]_{\mathbf{2a}}$ (M)	$[\mathbf{3i}]_0$ (M)	$[e]_{\mathbf{3i}}$ (M)	$[Pd(OAc)_2]_0$ (M)	$[KHCO_3]_0$ (M)
standard	0.34	0.51	0.17	1.36	1.02	0.034	0.34
same-excess	0.17	0.34	0.17	1.19	1.02	0.034	0.17

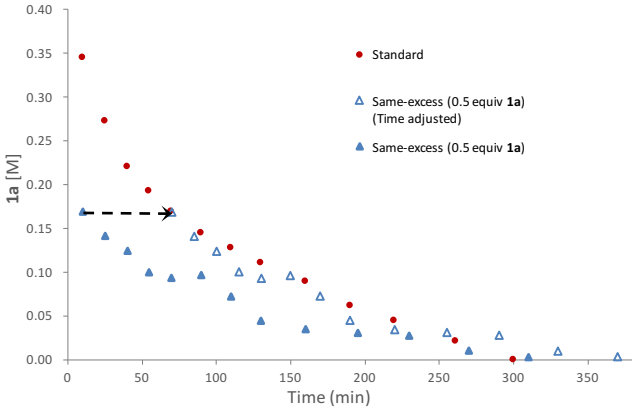

B

	$[\mathbf{1a}]_0$ (M)	$[\mathbf{2a}]_0$ (M)	$[\mathbf{3i}]_0$ (M)	$[Pd(OAc)_2]_0$ (M)	$[KHCO_3]_0$ (M)
Standard	0.34	0.51	1.36	0.034	0.34
different-excess $Pd(OAc)_2$	0.34	0.51	1.36	0.051	0.34

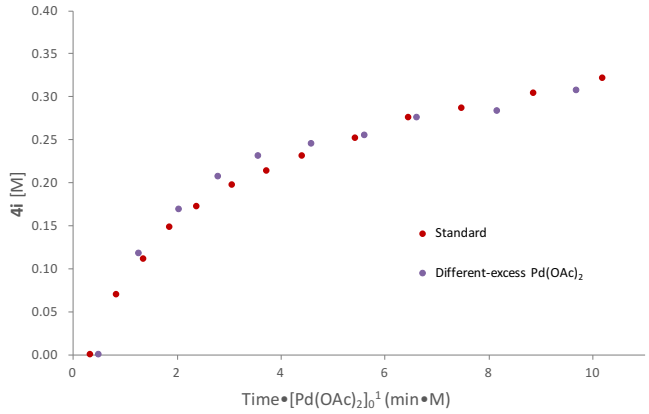

C

	$[\mathbf{1a}]_0$ (M)	$[\mathbf{2a}]_0$ (M)	$[e]_{\mathbf{2a}}$ (M)	$[\mathbf{3i}]_0$ (M)	$[e]_{\mathbf{3i}}$ (M)	$[Pd(OAc)_2]_0$ (M)	$[KHCO_3]_0$ (M)
standard	0.34	0.51	0.17	1.36	1.02	0.034	0.34
different-excess 2a	0.34	0.68	0.34	1.36	1.02	0.034	0.34
different-excess 3i	0.34	0.51	0.17	1.02	0.68	0.034	0.34
different-excess 1a	0.24	0.51	0.27	1.36	1.12	0.034	0.34

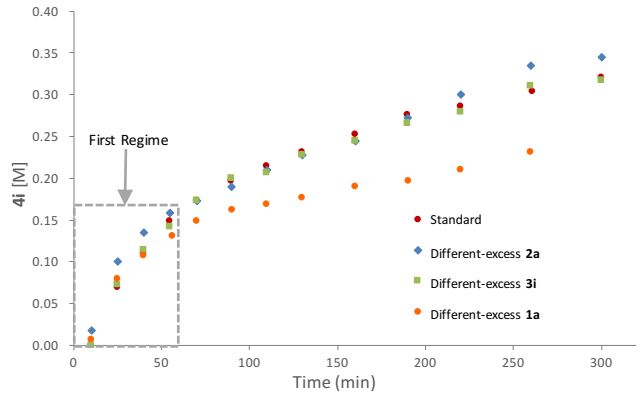

Figure 1. (A) Same-excess experiments start with 50% of substrate **1a**. (B) and (C) Different-excess experiments of phthalimide **2a**, **3i** and **1a**.

In order to determine the orders of the reaction components, a series of different-excess experiments were next performed. With higher concentration of $Pd(OAc)_2$, the reaction rate increased. By visualizing this data using the Burés method in which product formation is plotted using a normalized time axis, $t\bullet[Pd(OAc)_2]^1$, we find that there is overlay between the two rate profiles, indicating first-order kinetics in $[Pd(OAc)_2]$ (Figure 1B).[20] Changing the concentration of phthalimide (**2a**) and alkenyl iodide **3i** did not change the reaction rate, indicating apparent zero-order kinetic in both the [**2a**] and [**3i**]. Finally, changing the amount of alkene substrate **1a** did not change the reaction rate at low conversion, indicating apparent zero-order kinetics in [**1a**] as well (Figure 1C). Two possible mechanistic scenarios fit this kinetic data: (1) C–C reductive elimination from Pd(IV) is rate-limiting, or (2) oxidative addition is rate-determining, and the catalyst resting state is the nucleopalladated [Pd(II)–alkenyl iodide] dative complex (*vide infra*) under saturation kinetics. To distinguish between these two possibilities, a series of competition experiments and computational studies were undertaken.

To gain a quantitative understanding of the electrophile reactivity trends in Table 2, we designed several competition experiments (Scheme 5). We first examined the relative rates of two representative pairs of electrophiles by using equimolar quantities of the electrophiles of interest in a single flask and stopping the reactions at abridged times to measure initial rates. In Scheme 5A, the reactivity of alkenyl and aryl iodides was compared; 2 equiv of each of **3i** and **3q** were subjected to standard condition, and products **4i**/**4q** were formed in a >30:1 ratio. In Scheme 5B, the reactivity of two aryl iodides with different electronic properties was measured; in this case, 6 equiv of each of **3q** and **3p** were used, and products **4q**/**4p** were formed in a 2.5:1 ratio. Next, the global rates of these three different electrophiles were compared. The rate data for **3i** is shown in Figure 1. The rate profiles of aryl iodides **3q** and **3p** were measured following an analogous procedure (see Supporting Information). Initial rates of these three electrophiles were then compared. With aryl iodides, the carboamination reaction was substantially slower. The calculated k_{rel} values across this across this series of electrophiles (**3i**:**3q**:**3p**) is 71:2.2:1. This result indicates that alkenyl iodide **3i** reacts faster than both aryl iodides tested. Between the two aryl iodides, electron-rich aryl iodide **3q** is more reactive than electron-poor aryl iodide **3p**. The influence of the aryl iodide electronic properties on reaction rate is consistent with a rate-limiting C–C reductive elimination step, whereas the opposite trend would be expected if oxidative addition were rate-limiting.

Scheme 5. Competition Experiments

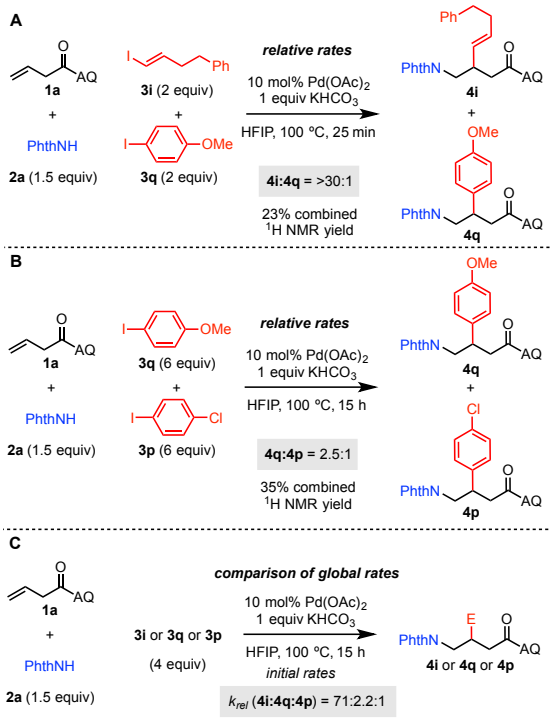

To elucidate the origin of the empirically observed reactivity trends, we performed a systematic computational investigation with various carbon electrophiles. Although the oxidative addition/reductive elimination processes involving Pd(0)/Pd(II) species have been extensively studied,[21] little mechanistic information about Pd(II)/Pd(IV) systems has been disclosed by computations.[22] C–C bond-forming reactions involving palladium(IV) intermediates are expected to furnish distinct reactivities, in particular, in promoting reductive elimination from a high-valent palladium center.[8a-d] However, the effects of the steric and electronic properties of carbon electrophiles in the C–C bond formation event have not been investigated systematically.

We performed density functional theory (DFT) calculations[23] on the oxidative addition (**TS1**) and reductive elimination (**TS2**) transition states of alkylpalladium(II) intermediate **9** reacting with various carbon electrophiles (Figure 2).[24] The computationally predicted activation Gibbs free energies agree well with the experimental reactivity trend that electron-rich aryl iodides are slightly more reactive than electron-poor aryl iodides and alkenyl iodides are among the most reactive substrates for the carboamination. Interestingly, in all reactions tested, the C–C reductive elimination[25] from the high-valent Pd(IV) species requires higher barrier than oxidative addition (Figure 3 and Figure S12 in the SI), indicating the steric properties of electrophiles will affect their reactivities. Indeed, the reactions with aryl iodides (**3o-3q** and **3z**) have higher barriers to reductive elimination than those with styrenyl and alkenyl iodides (**3a**, **3i**, and **3k**) due to greater steric repulsions about the forming C–Ar bond. This unfavorable interaction is evidenced by the short distance between the hydrogen atom on the alkyl group and the *ortho* carbon on the aryl group (2.37 Å) in the reductive elimination transition states (**TS2o** and **TS2q**). In contrast, the steric repulsions with the less hindered styrenyl and alkenyl groups are weaker, leading to much lower barriers in the reductive elimination (**TS2a**, **TS2i**, and **TS2k**). The barriers to reductive elimination are moderately sensitive to electronic effects. Electron-rich aryl iodides (e.g. **3q**) are more reactive in the rate-determining reductive elimination process. These results indicate that the aryl group can be considered as the nucleophilic component in the C–C reductive elimination step.[22a,22f]

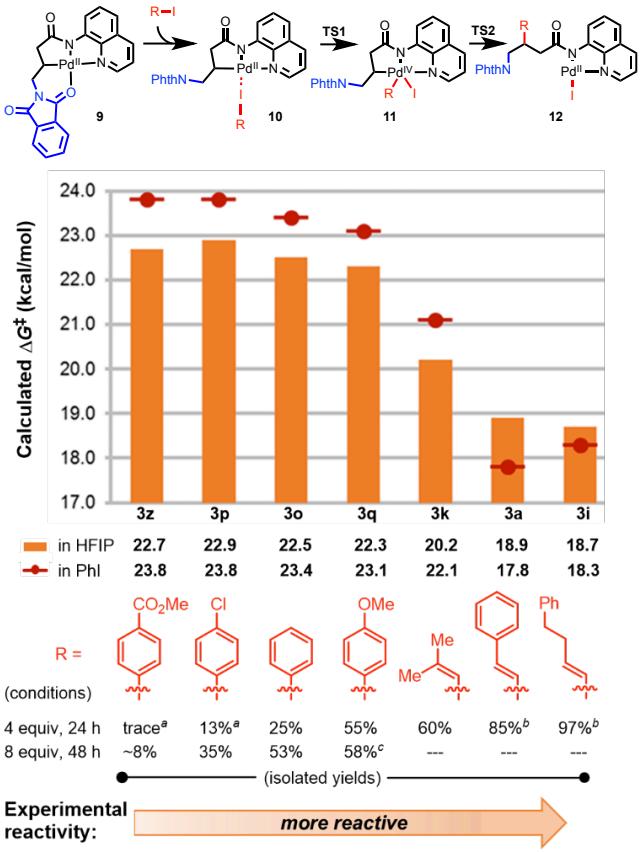

Figure 2. Computationally predicted reactivity trend of carbon electrophiles. The Gibbs free energies of activation are calculated from the catalyst resting state (in HFIP:**10** in the reaction with **3a** and **3i**, **9** in other reactions; in PhI: **10** in the reaction with **3i**, **9** in other reactions) to the rate-determining reductive elimination transition state (**TS2**). See Figure 3 and the SI for the energy profiles of the oxidative addition and reductive elimination steps. [a]Yields were determined by ^{1}H NMR analysis of the crude reaction mixture using CH_2Br_2 as internal standard. [b]Reaction run for 8 h. [c]Reaction run for 24 h.

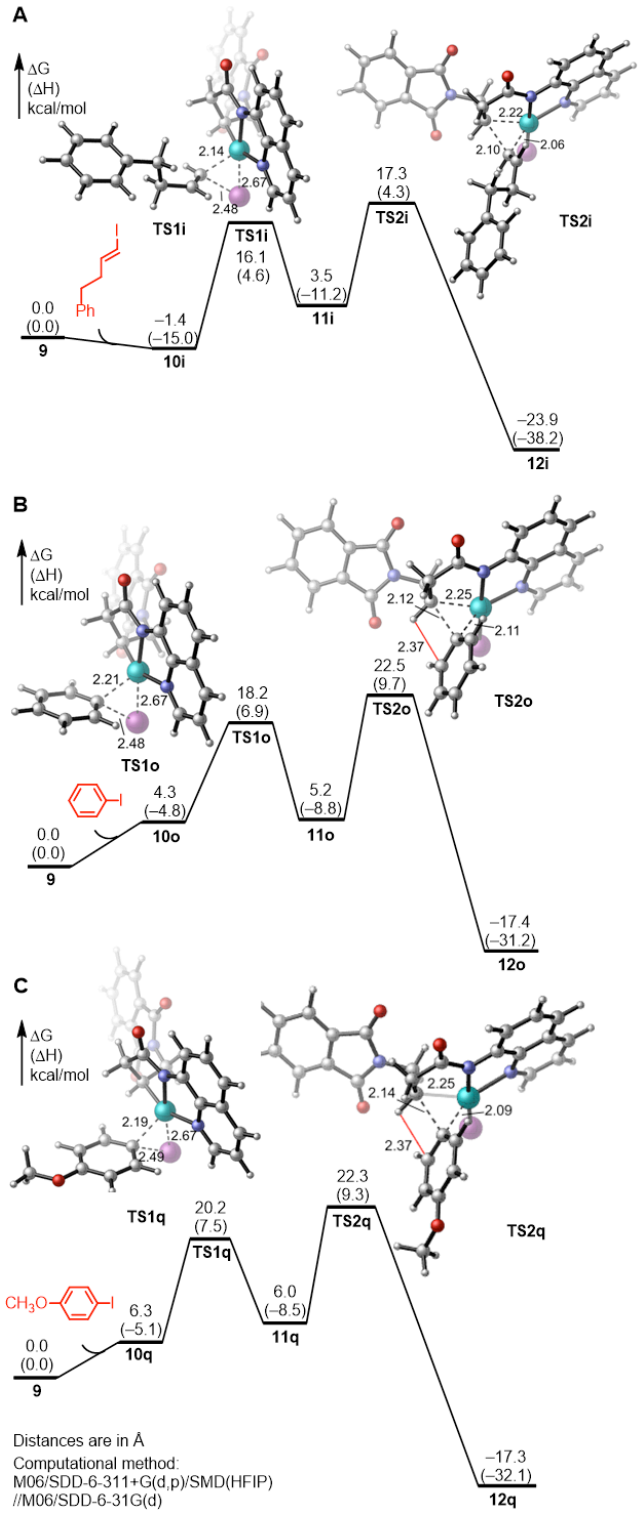

Figure 3. Computed reaction energy profiles of **9** with a) **3i**, b) **3o**, and c) **3q**. See SI for reactions with other electrophiles.

A plausible mechanism for this Pd(II)-catalyzed three-component alkene carboamination reaction is proposed in Scheme 6. To begin, the palladium catalyst, $Pd(OAc)_2$, coordinates with the AQ directing group of the substrate, bringing it in close proximity to the alkene. π-Lewis acid activation enables attack of the nitrogen nucleophile (e.g., phthalimide) on the backside of the Pd(II)-bound alkene (*anti*-nucleopalladation) to generate the alkylpalladium(II) species. This palladacycle does not undergo β-hydride elimination due to the stability and conformational rigidity imparted by the bidentate AQ directing group. Instead, it is sufficiently long-lived to be intercepted by a carbon electrophile via oxidative addition to form a palladium(IV) intermediate. Finally, stereoretentive C–C reductive elimination from the high-valent palladium center furnishes the palladium(II)–product complex. The computational data suggests that oxidative addition/C–I reductive elimination is reversible and that C–C reductive elimination is the rate-determining step. For electrophiles in which reductive elimination is particularly slow (*e.g.*, an electron-poor ArI), protodepalladation becomes a competitive non-desired pathway, leading to consumption of the starting material and diminished yields. Ligand exchange of this palladium(II)–product complex with a new substrate molecule then releases the 1,2-carboaminated product and regenerates the active palladium(II)–substrate complex.

Scheme 6. Proposed Reaction Mechanism

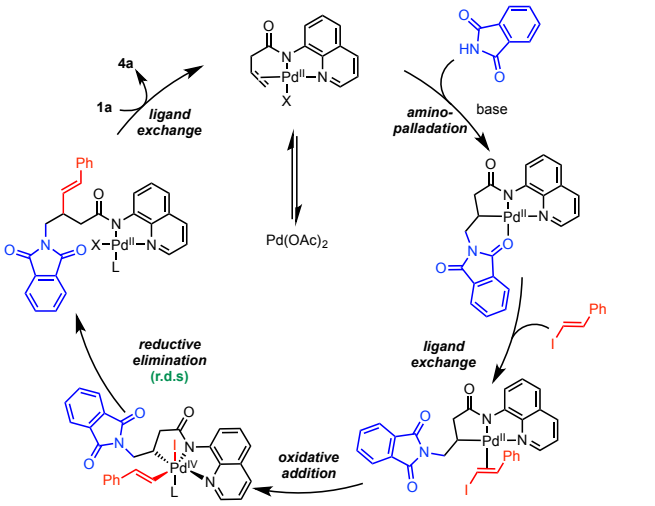

CONCLUSION

In conclusion, we have developed a regiocontrolled intermolecular carboamination reaction of unactivated alkenes using a removable 8-aminoquinoline directing group. By intercepting a chelation-stabilized aminopalladated intermediate with a carbon electrophile, this reaction has allowed us to achieve the first example of catalytic three-component carboamination of 3-butenoic acid derivatives. The reaction proceeded smoothly with a broad range of nitrogen nucleophiles, carbon electrophiles, and alkene substrates. Notable, several azaheterocycles relevant to medicinal chemistry were reactive, methyl iodide was a competent electrophile (enabling 1,2-aminomethylation), and sterically hindered internal and α-substituted alkene substrates participated in the reaction. The method was amenable to scale up for preparative chemistry. In particular, this transformation was used to convert a single alkene starting material into five drug molecules/derivatives containing a γ-amino acid or γ-lactam structural motifs. RPKA experiments elucidated the details of the reaction mechanism, pointing to C–C reductive elimination from a Pd(IV) center as the rate-determining step. DFT studies shed light on key elementary steps in the catalytic cycle and clarified the origins of the reactivity trends of different carbon electrophiles. Future investigation will focus on developing an asymmetric variant of this transformation. These results will be reported in due course.

ASSOCIATED CONTENT

Supporting Information

Experiment details, spectra data, copies of ^{1}H and ^{13}C NMR spectra, X-ray crystallographic data, and computational details. These materials are available free of charge via the Internet at http://pubs.acs.org.

AUTHOR INFORMATION

Corresponding Author

* E-mail: pengliu@pitt.edu, keary@scripps.edu

Notes

The authors declare no competing financial interest.

ACKNOWLEDGMENT

This work was financially supported by TSRI, Pfizer, Inc and the NSF (CHE-1654122). We gratefully acknowledge the Nankai University College of Chemistry for an International Research Scholarship (Z.W.). We thank Prof. Donna G. Blackmond for guidance with RPKA experiments, Dr. Milan Gembicky (UCSD) for X-ray crystallographic analysis, and Dr. Zachary K. Wickens (Harvard University) for helpful discussion. Materia, Inc. is acknowledged for generous donation of Hoveyda–Grubbs second-generation catalyst. We thank the NSF XSEDE for supercomputer resources.

REFERENCES

(1) (a) Kibayashi, C. *Chem. Pharm. Bull.* **2005**, *53*, 1375–1386. (b) Vitaku, E.; Smith, D. T.; Njardarson, J. T. *J. Med. Chem.* **2014**, *57*, 10257–10274.

(2) For selected examples of palladium(0)-catalyzed alkene carboamination involving intramolecular aminocyclization, see: (a) Ney, J. E.; Wolfe, J. P. *Angew. Chem. Int. Ed.* **2004,** *43*, 3605–3608. (b) Lira, R.; Wolfe, J. P. *J. Am. Chem. Soc.* **2004**, *126*, 13906–13907. (c) Mai, D. N.; Wolfe, J. P. *J. Am. Chem. Soc.* **2010**, *132*, 12157–12159. (d) Babij, N. R.; Wolfe, J. P. *Angew. Chem. Int. Ed.* **2013**, *52*, 9247–9250. (e) Faulkner, A.; Scott, J. S.; Bower, J. F. *J. Am. Chem. Soc.* **2015**, *137*, 7224–7230. (f) Orcel, U.; Waser, J. *Angew. Chem. Int. Ed.* **2016,** *55*, 12881–12885. For related examples involving Pd(II)/Pd(IV) catalysis, see: (g) Rosewall, C. F.; Sibbald, P. A.; Liskin, D. V.; Michael, F. E. *J. Am. Chem. Soc.* **2009**, *131*, 9488–9489. (h) Sibbald, P. A.; Rosewall, C. F.; Swartz, R. D.; Michael, F. E. *J. Am. Chem. Soc.* **2009**, *131*, 15945–15951. For selected examples of copper-catalyzed intramolecular carboamination, see: (i) Zeng, W.; Chemler, S. R. *J. Am. Chem. Soc.* **2007**, *129*, 12948–12949. (j) Miao, L.; Haque, I.; Manzoni, M. R.; Tham, W. S.; Chemler, S. R. *Org. Lett.* **2010**, *12*, 4739–4741. (k) Liwosz, T. W.; Chemler, S. R. *J. Am. Chem. Soc.* **2012**, *134*, 2020–2023. For selected examples of gold-catalyzed intramolecular carboamination, see: (l) Zhang, G.; Cui, L.; Wang, Y.; Zhang, L. *J. Am. Chem. Soc.* **2010**, *132*, 1474–1475. (m) Brenzovich, W. E., Jr.; Benitez, D.; Lackner, A. D.; Shunatona, H. P.; Tkatchouk, E.; Goddard, W. A., III; Toste, F. D. *Angew. Chem. Int. Ed.* **2010**, *49*, 5519–5522. For intramolecular aminocyanation, see: (n) Miyazaki, Y.; Ohta, N.; Semba, K.; Nakao, Y. *J. Am. Chem. Soc.* **2014**, *136*, 3732–3735. (o) Pan, Z.; Pound, S. M.; Rondla, N. R.; Douglas, C. J. *Angew. Chem. Int. Ed.* **2014**, *53*, 5170–5174.

(3) For two-component intermolecular carboamination using N–O reagents, see: (a) Piou, T.; Rovis, T. *Nature* **2015,** *527*, 86–90. (b) Hu, Z.; Tong, X.; Liu G. *Org. Lett.* **2016**, *18*, 1702–1705. (c) Lerchen, A.; Knecht, T.; Daniliuc, C. G.; Glorius, F. *Angew. Chem. Int. Ed.* **2016,** *55*, 15166–15170. For palladium(II)-catalyzed two-component carboamination of dienes, see: (d) Houlden, C. E.; Bailey, C. D.; Ford, J. G.; Gagné, M. R.; Lloyd-Jones, G. C.; Booker-Milburn, K. I. *J. Am. Chem. Soc.* **2008**, *130*, 10066–10067. For two- and three-component carboamination of conjugated alkenes involving the addition of carbon-centered radicals, see: (e) Um, C.; Chemler, S. R. *Org. Lett.* **2016**, *18*, 2515–2518. (f) Liu, Y.-Y.; Yang, X.-H.; Song, R.-J.; Luo, S.; Li, J.-H. *Nat. Commun.* **2017**, *8*, 14720.

(4) During the preparation of this manuscript, a copper-catalyzed enantioselective three-component carboamination of styrenes with *N*-fluoro sulfonamides and aryl boronic acids was reported: Wang, D.; Wu, L.; Wang, F.; Wan, X.; Chen, P.; Lin, Z.; Liu, G. *J. Am. Chem. Soc.* **2017**, *139*, 6811–6814.

(5) Gurak, J. A., Jr.; Yang, K. S.; Liu, Z.; Engle, K. M. *J. Am. Chem. Soc.* **2016**, *138*, 5805–5808.

(6) Yang, K. S.; Gurak, J. A., Jr.; Liu, Z.; Engle, K. M. *J. Am. Chem. Soc.* **2016**, *138*, 14705–14712.

(7) Liu, Z.; Zeng, T.; Yang, K. S.; Engle, K. M. *J. Am. Chem. Soc.* **2016**, *138*, 15122–15125.

(8) For reviews on high-valent palladium in catalysis, see: (a) Muñiz, K. *Angew. Chem. Int. Ed.* **2009,** *48*, 9412–9423. (b) Canty, A. J. *Dalton. Trans.* **2009**, 10409–10417. (c) Xu, L.-M.; Li, B.-J.; Yang, Z.; Shi, Z.-J. *Chem. Soc. Rev.* **2010**, *39*, 712–733. (d) Hickman, A. J.; Sanford, M. S. *Nature* **2012,** *484*, 177–185. For representative reviews on palladium-catalyzed alkene difunctionalization, see: (e) Jensen, K. H.; Sigman, M. S. *Org. Biomol. Chem.* **2008**, *6*, 4083–4088. (f) McDonald, R. I.; Liu, G.; Stahl, S. S. *Chem. Rev.* **2011**, *111*, 2981–3019. (g) Yin, G.; Mu, X.; Liu, G. *Acc. Chem. Res.* **2016**, *49*, 2413–2423. For other directing group approaches to alkene 1,2-difunctionalization via Pd(II)/Pd(IV) catalysis, see: (h) Neufeldt, S. R.; Sanford, M. S. *Org. Lett.* **2013**, *15*, 46–49. (i) Talbot, E. P. A.; Fernandes, T. d. A.; McKenna, J. M.; Toste, F. D. *J. Am. Chem. Soc.* **2014**, *136*, 4101–4104.

(9) For examples of intercepting alkylpalladium(II) intermediates with carbon electrophiles in C–H activation, see: (a) Zaitsev, V. G.; Shabashov, D.; Daugulis, O. *J. Am. Chem. Soc.* **2005**, *127*, 13154–13155. (b) Shabashov, D.; Daugulis, O. *J. Am. Chem. Soc.* **2010**, *132*, 3965–3972. (c) Ano, Y.; Tobisu, M.; Chatani, N. *J. Am. Chem. Soc.* **2011**, *133*, 12984–12986. (d) Gutekunst, W. R.; Baran, P. S. *J. Org. Chem.* **2014**, *79*, 2430–2452. For representative reviews, see: (e) He J.; Wasa, M.; Chan, K. S. L.; Shao, Q.; Yu, J.-Q. *Chem. Rev.* **2017**, *117*, 8754–8786. (f) Daugulis, O.; Roane, J.; Tran, L. D. *Acc. Chem. Res.* **2015**, *48*, 1053–1064.

(10) For an example of palladium(II)-catalyzed intermolecular aminocarbonylation of alkenes, see: (a) Cheng, J.; Qi, X.; Li, M.; Chen, P.; Liu, G. *J. Am. Chem. Soc.* **2015**, *137*, 2480–2483. For intermolecular carboazidation of alkenes, see: (b) Weidner, K.; Giroult, A.; Panchaud, P.; Renaud, P. *J. Am. Chem. Soc.* **2010**, *132*, 17511–17515. For intermolecular aminocyanation of alkenes, see: (c) Zhang, H.; Pu, W.; Xiong, T.; Li, Y.; Zhou, X.; Sun, K.; Liu, Q.; Zhang, Q. *Angew. Chem. Int. Ed.* **2013**, *52*, 2529–2533.

(11) This alkene *Z*/*E* isomerization phenomenon was previously observed in a C–H alkenylation reaction: Shan, G.; Huang, G.; Rao, Y. *Org. Biomol. Chem.* **2015**, *13*, 697–701. In this report, the authors proposed a *Z*/*E* isomerization pathway via an Pd(IV)-π-benzyl-type intermediate when using (*Z*)-styrenyl iodide as the electrophile. However, this model cannot explain the isomerization of (*Z*)-alkenyl iodide bearing an alkyl group (for example **4j** in the present work). We have found that when *Z*-alkenyl iodides are employed in the reaction, the corresponding *E* isomer is not observed under the reaction conditions. We have further established that reaction rates with *E*- and *Z*-alkenyl iodides are similar (with in a factor of 2), which is inconsistent with a scenario in which the Z-isomer is converted to *E*, which in turn reacts with a sufficiently high rate such that it cannot be detected. Beyond these preliminary insights, the mechanism by which *Z*/*E*-isomerization takes place remains unclear.

(12) When (*E*)-*N*-(quinolin-8-yl)pent-3-enamide (**1b**) was exposed to the reaction conditions in the absence of nucleophile and electrophile, *E*/*Z* isomerization of **1b** was observed; after 40 h, the *E*/*Z* ratio was approximately 2.9:1 based on ^{1}H NMR analysis.

(13) (a) Attal, N.; Cruccu, G.; Baron, R.; Haanpää, M.; Hansson, P.; Jensen, T. S.; Nurmikko, T. *Eur. J. Neurol.* **2010**, *17*, 1113–1123. (b) Wensel, T. M.; Powe, K. W.; Cates, M. E. *Ann. Pharmacother.* **2012**, *46*, 424–429.

(14) Mann, A.; Boulanger, T.; Brandau, B.; Durant, F.; Evrard, G.; Heaulme, M.; Desaulles, E.; Wermuth, C. G. *J. Med. Chem.* **1991**, *34*, 1307–1313.

(15) Sytinsky, I. A.; Soldatentkov, A. T.; Lajtha, A. *Prog. Neurobiol.* **1978**, *10*, 89–133.

(16) Griswold, D. E.; Webb, E. F.; Breton, J.; White, J. R.; Marshall, P. J.; Torphy, T. J. *Inflammation* **1993**, *17*, 333–344.
(17) Substrate **8** has been found to undergo this C–H alkenylation reaction under a different condition in moderate yield, see Ref. 11.
(18) (a) Blackmond, D. G. *Angew. Chem. Int. Ed.* **2005**, *44*, 4302–4320. (b) Mathew, J. S.; Klussmann, M.; Iwamura, H.; Valera, F.; Futran, A.; Emanuelsson, E. A. C.; Blackmond, D. G. *J. Org. Chem.* **2006**, *71*, 4711–4722. (c) Blackmond, D. G. *J. Am. Chem. Soc.* **2015**, *137*, 10852–10866.
(19) This complex persists throughout the course of the reaction, and by ^{1}H NMR integration, it appears to account for most of the Pd(II) in solution. It is unclear, however, if this species is the catalyst resting state because the reaction aliquots are cooled to room temperature and diluted into $CDCl_3$ prior to analysis. If any steps in the catalytic cycle are reversible, then the distribution of Pd(II) species at equilibrium could be different under the analysis conditions and the reaction conditions. The reaction mixture could not be directly monitored by ^{1}H NMR under the reaction conditions for technical reasons.
(20) Burés, J. *Angew. Chem. Int. Ed.* **2016**, *55*, 2028–2031.
(21) For reviews: (a) Hartwig, J. F. *Organotransition Metal Chemistry: from Bonding to Catalysis*; University Science Books: Sausalito, 2009. (b) Hartwig, J. F. *Inorg. Chem.* **2007**, *46*, 1936–1947. (c) Xue, L.; Lin, Z., *Chem. Soc. Rev.* **2010**, *39*, 1692–1705. (d) Bonney, K. J.; Schoenebeck, F. *Chem. Soc. Rev.* **2014**, *43*, 6609–6638. For computational studies on the C–C bond forming reductive elimination from palladium(II): (e) Ananikov, V. P.; Musaev, D. G.; Morokuma, K. *Organometallics* **2005**, *24*, 715–723. (f) Pérez-Rodríguez, M.; Braga, A. A. C.; Garcia-Melchor, M.; Pérez-Temprano, M. H.; Casares, J. A.; Ujaque, G.; de Lera, A. R.; Alvarez, R.; Maseras, F.; Espinet, P. *J. Am. Chem. Soc.* **2009**, *131*, 3650DFT–3657. For experimental studies on the C–C bond forming reductive elimination from palladium(II): (g) Culkin, D. A.; Hartwig, J. F. *Organometallics* **2004**, *23*, 3398–3416. (h) Klinkenberg, J. L.; Hartwig, J. F. *J. Am. Chem. Soc.* **2012**, *134*, 5758–5761.
(22) For computational studies of C–C and C–X reductive elimination from palladium(IV) center, see: (a) Fu, Y.; Li, Z.; Liang, S.; Guo, Q. X.; Liu, L. *Organometallics*, **2008**, *27*, 3736–3742. (b) Ball, N. D.; Gary, J. B.; Ye, Y.; Sanford, M. S. *J. Am. Chem. Soc.* **2011**, *133*, 7577–7584. (c) Dang, Y.; Qu, S.; Nelson, J. W.; Pham, H. D.; Wang, Z. X.; Wang, X. *J. Am. Chem. Soc.* **2015**, *137*, 2006–2014. (d) Pendleton, I. M.; Perez-Temprano, M. H.; Sanford, M. S.; Zimmerman, P. M. *J. Am. Chem. Soc.* **2016**, *138*, 6049–6060. (e) Canty, A. J.; Ariafard, A.; Camasso, N. M.; Higgs, A. T.; Yates, B. F.; Sanford, M. S. *Dalton Trans.* **2017**, *46*, 3742–3748. For selected experimental studies, see: (f) Racowski, J. M.; Dick, A. R.; Sanford, M. S. *J. Am. Chem. Soc.* **2009**, *131*, 10974–10983. (g) Ball, N. D.; Kampf, J. W.; Sanford, M. S. *J. Am. Chem. Soc.* **2010**, *132*, 2878–2879. (h) Oloo, W.; Zavalij, P. Y.; Zhang, J.; Khaskin, E.; Vedernikov, A. N. *J. Am. Chem. Soc.* **2010**, *132*, 14400–14402. (i) Camasso, N. M.; Perez-Temprano, M. H.; Sanford, M. S. *J. Am. Chem. Soc.* **2014**, *136*, 12771–12775.
(23) DFT calculations were performed using Gaussian 09, Revision D.01, Frisch, M. J.; Trucks, G. W.; Schlegel, H. B.; Scuseria, G. E.; Robb, M. A.; Cheeseman, J. R.; Scalmani, G.; Barone, V.; Mennucci, B.; Petersson, G. A.; Nakatsuji, H.; Caricato, M.; Li, X.; Hratchian, H. P.; Izmaylov, A. F.; Bloino, J.; Zheng, G.; Sonnenberg, J. L.; Hada, M.; Ehara, M.; Toyota, K.; Fukuda, R.; Hasegawa, J.; Ishida, M.; Nakajima, T.; Honda, Y.; Kitao, O.; Nakai, H.; Vreven, T.; Montgomery, J. A.; Peralta, J. E., Jr.; Ogliaro, F.; Bearpark, M.; Heyd, J. J.; Brothers, E.; Kudin, K. N.; Staroverov, V. N.; Kobayashi, R.; Normand, J.; Raghavachari, K.; Rendell, A.; Burant, J. C.; Iyengar, S. S.; Tomasi, J.; Cossi, M.; Rega, N.; Millam, J. M.; Klene, M.; Knox, J. E.; Cross, J. B.; Bakken, V.; Adamo, C.; Jaramillo, J.; Gomperts, R.; Stratmann, R. E.; Yazyev, O.; Austin, A. J.; Cammi, R.; Pomelli, C.; Ochterski, J. W.; Martin, R. L.; Morokuma, K.; Zakrzewski, V. G.; Voth, G. A.; Salvador, P.; Dannenberg, J. J.; Dapprich, S.; Daniels, A. D.; Farkas, Ö.; Foresman, J. B.; Ortiz, J. V.; Cioslowski, J. and Fox, D. J. Gaussian, Inc., Wallingford CT, 2009. Geometry optimization was performed using M06 and the SDD basis set for Pd/I and 6-31G(d) for other atoms. Single point calculations were performed using M06 and the SDD basis set for Pd/I and 6-311+G(d,p) for other atoms. Solvation energy corrections were calculated using the SMD solvation model in both HFIP (ε = 16.7) and PhI (ε = 4.547) solvents. Although HFIP was used experimentally as solvent, the reaction medium is expected to be less polar than pure HFIP when large quantities of aryl or alkenyl iodide electrophiles are used. The calculations in the two different solvents indicate that the electronic effects of aryl iodides are slightly stronger in the less polar solvent (PhI), while the greater reactivities of alkenyl and styrenyl iodides are observed in both solvents.
(24) The entire catalytic cycle has been computed, and reductive elimination was found to be the rate-limiting step with all of the electrophiles shown in Figure 2. Figure 3 and the Supporting Information contain details for the oxidative addition and reductive elimination steps with different electrophiles. The details for the other steps will be published in a separate manuscript in due course.
(25) An alternative reductive elimination process involving cationic Pd(IV) species formed after the dissociation of I^- from **11** was ruled out by DFT calculations. See SI for details.

TOC Image